Magnetic and structural studies on two-dimensional antiferromagnets (MCl)LaNbO (M = Mn, Co, Cr)

AUTHOR(S):

Kitada, Atsushi; Tsujimoto, Yoshihiro; Nishi, Masakazu; Matsuo, Akira; Kindo, Koichi; Ueda, Yutaka; Ajiro, Yoshitami; Kageyama, Hiroshi

CITATION:

Kitada, Atsushi ...[et al]. Magnetic and structural studies on two-dimensional antiferromagnets (MCl)LaNbO (M = Mn, Co, Cr). Journal of the Physical Society of Japan 2016, 85(3): 034005.

ISSUE DATE:

2016-03-15

URL:

http://hdl.handle.net/2433/259842

Magnetic and Structural Studies on Two-dimensional Antiferromagnets (*M*Cl)$LaNb_2O_7$ (*M* = Mn, Co, Cr)

Atsushi Kitada[1*], Yoshihiro Tsujimoto[1,2], Masakazu Nishi[3], Akira Matsuo[3], Koichi Kindo[3], Yutaka Ueda[3,4], Yoshitami Ajiro[1], and Hiroshi Kageyama[1,5†]

[1] *Department of Energy and Hydrocarbon Chemistry, Graduate School of Engineering, Kyoto University, Nishikyo, Kyoto 615-8510, Japan*

[2] Materials Processing Unit, *National Institute for Materials Science (NIMS), Tsukuba, Ibaraki 305-0047, Japan*

[3] *Institute for Solid State Physics, University of Tokyo, Kashiwa, Chiba 277-8581, Japan*

[4] *Toyota Physical and Chemical Research Institute, Nagakute, Aichi 480-1192, Japan*

[5] *CREST, Japan Science and Technology Agency (JST), Kawaguchi, Saitama 332-0012, Japan*

*current address: *Department of Materials Science and Engineering, Kyoto University, Sakyo, Kyoto 606-8501, Japan*; E-mail: kitada.atsushi.3r@kyoto-u.ac.jp

†E-mail: kage@scl.kyoto-u.ac.jp

We report magnetic and structural studies on the two-dimensional antiferromagnets

(*M*Cl)$LaNb_2O_7$ (*M* = Mn, Cr, Co), prepared by topochemical reactions of a layered perovskite $RbLaNb_2O_7$. Electron diffraction of these oxyhalides revealed a superstructure with a $\sqrt{2}a \times \sqrt{2}a$ cell for *M* = Mn and Co, and a $2a \times 2a$ cell for *M* = Cr, indicating that the *M*Cl networks are distorted from an ideal square lattice. Neutron diffraction experiments showed that *M* = Mn and Co exhibit a (π 0 π) antiferromagnetic order as observed for the *S* = 1/2 counterparts. (CoCl)$LaNb_2O_7$ with a strong spin anisotropy shows an antiferro to weak-ferromagnetic transition at low field, followed by novel two-step metamagnetic transitions likely associated with a 1/2 plateau for 27 T – 54 T. Possible spin structures under magnetic field are discussed in terms of an Ising-type model. By contrast, (CrCl)$LaNb_2O_7$ exhibits a (π π π) order, which is the first observation among related oxyhalides, and a spin-flop transition at 12 T due to a weak spin anisotropy. These results suggest that a slight difference in the *M*Cl structure and spin anisotropy provides a crucial influence on the magnetic properties.

1. Introduction

Two-dimensional (2D) frustrated spin systems have been a central subject in condensed matter physics for the past several decades because of various exotic phenomena they exhibit.[1)] Magnetic behaviors are different, depending on whether the system is quantum or classical. For example, in quantum triangular Heisenberg antiferromagnets, the ground-state wavefunction does not simply lead to the classical 120° structure, as a result of strongly enhanced quantum fluctuations.[2-6)]

The J_1-J_2 model is a frustrated 2D square lattice system consisting of first nearest neighbor and second-nearest-neighbor interactions. In the classical limit, three magnetically ordered states are expected to appear: a (π 0) AF state when $\alpha \equiv J_2/J_1$ is $-0.5 < \alpha < 0.5$ [Fig. 1(b)], a (π π) antiferromagnetic (AF) state when α ~~$\equiv J_2/J_1$~~ < 0.5 with $J_1 > 0$ [Fig. 1(c)], and a (0 0) ferromagnetic (FM) state when $\alpha < -0.5$ with $J_1 < 0$. In the quantum case, a spin-disordered state with a finite gap is proposed at the boundary between (π π) and (π 0) phases, where AF J_1 and AF J_2 compete.[7,8)] Subsequent theoretical investigations both in classical and quantum cases propose a spin nematic state at the boundary between the (π 0) and (0 0) FM phases, where FM J_1 and AF J_2 compete.[9~~8~~)] Hence, it is interesting and challenging to search for compounds of 2D frustrated spin systems, where nontrivial magnetic phenomena are observed.

The layered cupric oxyhalide $(CuCl)LaNb_2O_7$ and related cupric compounds were initially proposed as the quantum case of J_1-J_2 model. The compounds are featured by competing FM and AF interactions, and as a result exhibit various quantum behaviors including spin-singlet ground states in $(CuCl)LaNb_2O_7$ and $(CuCl)Ca_2Nb_3O_{10}$,[10-12] a $(\pi\ 0\ \pi)$ order in $(CuBr)LaNb_2O_7$[13] and $(CuCl)LaTa_2O_7$,[14] a 1/3 magnetization plateau in $(CuBr)A_2B_3O_{10}$,[15] and a gapless spin-disordered state in $(CuCl)Ca_2NaNb_4O_{13}$.[16] The early structural studies indicated that the copper-halide layer forms the ideal square lattice with the space group $P4/mmm$ [Fig. 1(a)].[10,13-15] However, the deviation from the ideal J_1-J_2 model was later indicated from various experiments.[17-21] For example, the NMR study revealed an orthorhombic distortion in $(CuBr)LaNb_2O_7$, resulting in distinct magnetic interactions along the a- and b-axes.[18] High resolution diffraction experiments on $(CuCl)LaNb_2O_7$ together with first principles calculations revealed a $2a \times 2b \times c$ orthorhombic cell with the strongest magnetic coupling for the 4th neighboring Cu-Cu ions.[19,20] The 1/3 magnetization plateau of $(CuBr)A_2B_3O_{10}$ was accounted for by introducing the 3rd nearest neighbor interaction J_3 to the J_1-J_2 model.[20]

Facing controversial interpretations on the magnetic properties of cupric oxyhalides, it is important to investigate $(M\mathrm{Cl})LaNb_2O_7$ (M = V, Cr, Mn, Fe, Co),[21] which expectedly have more classical states (S = 3/2 for M = V, Co; S = 2 for Cr and Fe; S = 5/2 for Mn). $(FeCl)LaNb_2O_7$ has a distorted FeCl network,[22,23] and exhibits $(\pi\ 0)$-type magnetic order[24] as observed in $(CuBr)LaNb_2O_7$. For Mn, Co and Cr, antiferromagnetic phase transitions are suggested from magnetic susceptibility and heat

capacity results.[26,27] For Co, strong uniaxial anisotropy is suggested from the Curie-Weiss fitting. Table I summarizes the values of Weiss temperature θ, Néel temperature T_N, and T^{χ}_{max},[23,26,27] where T^{χ}_{max} represents a temperature at which the susceptibility shows a broad maximum. Apparently, these quantities are not scaled with S.

To date, however, the magnetic structures of the Mn, Co and Cr materials have not yet been investigated. Equally important is to examine whether the MCl networks (M = Mn, Co, Cr) have structural distortions from the simple square lattice as in M = Cu[16,17,18,19,20] and Fe,[23,24] which should affect their magnetism. In this paper, we present structural and magnetic properties of (MnCl)$LaNb_2O_7$, (CoCl)$LaNb_2O_7$ and (CrCl)$LaNb_2O_7$ using electron diffraction (ED), neutron powder diffraction (NPD) and high-field magnetization measurements.

2. Experimental Procedure

Powder samples of (MCl)$LaNb_2O_7$ (M = Mn, Co, Cr) were synthesized via two-step ion exchange reactions described previously.[21,22] First, $RbLaNb_2O_7$ was prepared via conventional high temperature solid state reaction using Rb_2CO_3, La_2O_3 and Nb_2O_5 with a molar ratio of 1.25:1:2. $RbLaNb_2O_7$ was then mixed with $LiNO_3$ with a molar ratio of 1:10 and heated in air at 400 °C for 24 h, to yield $LiLaNb_2O_7$. Finally, $LiLaNb_2O_7$ was mixed with a two-molar excess of MCl_2 in an Ar-filled dry box (< 0.1 ppm H_2O/O_2), sealed in evacuated Pyrex tubes (< 4×10^{-2} Pa) and heated at around 400 °C for 7 days. The target compounds were isolated by washing the products with

water or ethanol and dried overnight at 120 °C. ED measurements were carried out at ambient temperature using a JEM2010F system with an operating voltage of 200 kV at the Institute for Solid State Physics (ISSP) at the University of Tokyo. The specimens were finely ground in methanol and then placed on Cu microgrids.

NPD experiments were conducted using the IMR-HERMES diffractometer (T1-3), installed at the JRR-3 reactor in Japan Atomic Energy Agency (JAEA), Tokai. Polycrystalline samples of (MnCl)$LaNb_2O_7$ (4.2 g), (CoCl)$LaNb_2O_7$ (6.6 g) and (CrCl)$LaNb_2O_7$ (4.9 g) were put into vanadium cylinders. Neutrons were monochromatized using a Ge(331) and the wavelengths were 1.82646 Å for Mn and Co and 1.8204 Å for Cr. The NPD patterns were simulated with RIETAN-2000 software.[~~27~~28] High-field magnetization measurements using a pulsed magnet installed at ISSP were conducted at 1.3 K for Co up to 56 T and at 4.2 K for Cr up to 50 T.

3. Results and Discussion

Room temperature X-ray diffraction studies indicated the tetragonal symmetry with cell constants: a = 3.899(3) Å, c = 12.04(5) Å for M = Mn, a = 3.908(1) Å, c = 11.63(4) Å for Co, and a = 3.899(6) Å, c = 11.97(5) Å for Cr, in good agreement with the previous results.[~~21~~22] However, ED studies at room temperature revealed superreflections in the *ab* plane. Figure 2 displays ED patterns along [001]. All the compounds show weak commensurate reflections, together with strong fundamental ones, explained by an enlarged unit cell of $\sqrt{2}a \times \sqrt{2}a$ for Mn and Co [Figs. 2(a) and 2(b)] and $2a \times 2a$ for Cr [Fig. 2(c)]. As reported in (CuCl)$LaNb_2O_7$,[~~18~~19,~~28~~29] the

observed superreflections are likely attributed to distortion in the *M*Cl networks combined with octahedral tilting in the perovskite slabs.

Shown in Fig. 3 are NPD patterns of (*M*Cl)$LaNb_2O_7$ (*M* = Mn, Co, Cr) at temperatures above and below T_N. The T_N values of these materials are listed in Table I. Unlike the ED experiments, no superreflections were observed in the NPD profiles above T_N because of low instrumental resolution. Below T_N, the NPD profiles clearly show additional diffraction peaks, indicating AF order. With increasing temperature, the intensities of these peaks decrease and only background is seen above T_N, confirming that these are magnetic reflections. Interestingly, the modulation wave vectors *q* are different between *M* = Mn, Co and *M* = Cr: the Mn and Co compounds have (π 0 π) while the Cr compound has (π π π). Figure 4 shows the temperature dependence of the (1/2 0 1/2) intensity for Mn, Co, and the (1/2 1/2 1/2) intensity for Cr. Consequently, the Mn and Co compounds have the similar (π 0) AF order as (CuBr)$LaNb_2O_7$,[~~12~~13] (CuCl)$LaTa_2O_7$,[~~13~~14] and (FeCl)$LaNb_2O_7$,[~~24~~25] while the Cr compound has the (π π) AF order. Notably, the (π π) order has not been reported so far in the related layered oxyhalides. The (π 0) and (π π) AF ordered states are predicted by the J_1-J_2 theory and observed experimentally in other square lattice spin systems, *e.g.*, (π 0) in $Li_2VO(Si, Ge)O_4$ and $BaCdVO(PO_4)_2$, [~~29~~30,~~30~~31] and (π π) in $VOMoO_4$.[~~31~~32]

As shown in Fig. 5, we simulated NPD patterns of (*M*Cl)$LaNb_2O_7$, assuming spin orientation parallel to the *c*-axis (upper panels) and *b*-axis (lower panels) and found that the *c*-axis spin orientation provided a better fit. We also tried other models with different spin orientations, but failed to obtain better results (not shown). The obtained *c*-axis

orientation in (MCl)$LaNb_2O_7$ differs from the b-axis orientation in (CuBr)$LaNb_2O_7$.[12,13] This spin orientation in (MnCl)$LaNb_2O_7$ may originate from the magnetic dipole-dipole interactions between Mn^{2+}(d^5) moments as in a 2D square lattice magnet K_2MnF_4.[32,33] In (CoCl)$LaNb_2O_7$ and (CrCl)$LaNb_2O_7$, the crystal field anisotropy toward the c-axis in MCl_4O_2 octahedra may help spins to align parallel to the c-axis. A similar behavior is observed in a 2D distorted square lattice magnet $CoCl_2 \cdot 2D_2O$, where each Co^{2+} ion is surrounded by four equatorial Cl^- ions and two apical O^{2-} ions and the Co moments point parallel to the apical oxygen direction.[33,34]

Using the low temperature NPD data for Mn and Cr, the magnetic moments were estimated, respectively, to be 4.5(2) μ_B and 3.7(2) μ_B, which are close to the ideal spin-only value (5 μ_B and 4 μ_B). In marked contrast, the magnetic moment for Co was approximately 3.5(1) μ_B, somewhat larger than the theoretically expected value of 3 μ_B in high spin state (Co^{2+}, d^7). This is consistent with the result of the Curie-Weiss fitting which yielded a larger effective magnetic moment than the theoretical value for S = 3/2.[26,27] On the assumption of the tetragonal crystal field for $CoCl_4O_2$ octahedron (when the ideal $P4/mmm$ structure is considered), the ground orbital state of Co^{2+} is a Kramers doublet with Ising-like anisotropy. Then, the observed magnetic moment gives the parallel g-value ($g_{//}$) of ~ 7.0(2) with a fictitious spin of J = 1/2.

It appears that the observed (π 0) and (π π) spin structures in the present compounds are consistent with the J_1-J_2 model. However, the ED observation of superstructures indicates a certain distortion of MCl network from the simple square lattice. Structural refinement and theoretical considerations of (CuCl)$LaNb_2O_7$ with the 2a × 2b

superstructure revealed that not only the distortion of the CuCl network but also the anisotropy derived from the active Cu $d(3x^2-r^2)$ orbital result in a system corresponding to the ferromagnetically-coupled Shastry-Sutherland model.[18,19,19,20,34,35] The observed difference in magnetic order between M = Cr and M = Mn, Co is likely to be associated with the different superstructures and d electron count (or orbital degree of freedom). The (π π) order in M = Cr may be discussed in terms of the square lattice J_1-J_2 model or the Shastry-Sutherland model. In the case of the former model, J_1 is antiferromagnetic and dominant over J_2. The latter model was derived to explain the magnetism of $(CuCl)LaNb_2O_7$,[18,19] in which the 4th nearest neighbor Cu-Cl-Cl-Cu super-superexchange interactions, J_4 is antiferromagnetic and dominant, while J_1 and J_2 are ferromagnetic and similar in magnitude, resulting in $|J_4| >> |J_1| \sim |J_2|$. Although the ($\pi$ π) order cannot be derived from the original model, a recent theory has shown that the (π π) phase is stabilized when J_1 and J_2 are treated independently.[34,35] A precise (super)structure of $(CrCl)LaNb_2O_7$ remains to be determined.

Figure 6(a) displays the magnetization curve of $(CoCl)LaNb_2O_7$ powder at 1.3 K. For $0 < H < 5$ T, there is a hysteresis in increasing and decreasing field, indicating the presence of an antiferromagnetic to weak-ferromagnetic phase with a ferromagnetic component M_{FM} of ~ 0.15 μ_B, which will be discussed later. At higher field, double-step metamagnetic transitions associated with the Ising-like anisotropy were observed at H_{c1} ~ 27 T and H_{c2} ~ 54 T. This magnetization behavior is quite different from those in S = 1 $(NiCl)Sr_2Ta_3O_{10}$ which shows a single-step spin-flop transition.[35,36] The total magnetization of the powder specimen should be described as M_{FM} + ($M_{//}$ + 2$M_{\perp}$)/3,

where $M_{//}$ and $M_{\perp}$ denote the magnetization parallel and perpendicular to the easy axis, respectively. We notice that the ratio H_{c1} : H_{c2} is 1:2, strongly indicating that each transition at H_{c1} and H_{c2} require the same energy. We suppose that $M_{//}$ has two jumps at H_{c1} and H_{c2} with the same height of about 0.6 μ_B, and the linear increase between 5 T and 27 T comes only from $M_{\perp}$. This hypothesis is schematically illustrated in Figs. 6(a) and 6(b). We note that the total increment in the magnetization due to two jumps is 1.2 μ_B, which is close to 1/3 of 3.5(1) μ_B, the average value for powder sample with $g_{//}$ = 7.0(2) and J = 1/2, as indicated by the NPD results. Then, the observed two jumps at H_{c1} and H_{c2} corresponds to a 1/2 magnetization plateau and the saturation for $M_{//}$. Taking into account the uniaxial spin anisotropy and the fact that $g\mu_B H_{c1}$ equals to $g\mu_B(H_{c2} - H_{c1})$, the 1/2 plateau is explained as follows. In Fig. 7(a), the (π 0) two-sublattice state with a zero magnetization is expressed as [○●○●○●○●…], where ○ and ● stand for spin-up and spin-down. The first transition at H_{c1} to the 1/2-plateau state with a four-sublattice [○○○●○○○●…] requires half of spin-down to be reversed. The second transition at H_{c2} to the saturated state [○○○○○○…] requires the rest spin-down to be reversed. Thus, the ratio of the critical field H_{c1} : H_{c2} = 1 : 2, which is consistent with the experimental result.

Similar metamagnetic transitions with a plateau are observed in a FM chain compound $CoCl_2 \cdot 2H_2O$ with the uniaxial spin anisotropy, of which interchain interactions are viewed as a 2D AF distorted square lattice magnet with strong anisotropy.[~~36~~37)] It is noted, however, that this compound has H_{c1} : H_{c2} = 2 : 3 with a 1/3 magnetization plateau. This is because the transition at H_{c1} from zero-magnetization

(two-sublattice [○●○●○●○●…]) to 1/3 plateau (three-sublattice [○○●○○●…]) needs double energy, compared to the transition at H_{c2} from 1/3 plateau [○○●○○●…] to saturation [○○○○○○…].

In (CoCl)$LaNb_2O_7$, the (π 0 π) state was observed at zero field. Since the AF out-of-plane interactions should be small from the structural viewpoint [Fig. 1(a)], weak magnetic field can easily change the (π 0 π) structure to the (π 0 0) structure. It is notable that the magnetization curve in $0 < H < 5$ T (= H_{FM}) has a FM-like hysteresis, with a finite residual magnetization when one extrapolates the magnetization curve between $H_{FM} < H < H_{c1}$ [Fig. 6(a)]. This suggests that above H_{FM}, (CoCl)$LaNb_2O_7$ has a weak ferromagnetic component of $M_{FM} \sim 0.15\ \mu_B$. Namely, at zero field, the in-plane canted AF layers provide no net magnetization since they are stacked in a staggered manner due to the small out-of-plane AF interactions. Above H_{FM}, by contrast, the canted layers are uniformly stacked to produce a net magnetization where M_{FM} overcome the out-of-plane AF interactions. Since the value of M_{FM} (0.15 μ_B) corresponds to around 4% of the saturated moment 3.5 μ_B, the magnitude of the out-of-plane AF interactions are around 4% of H_{FM}, i.e. only 0.2 T.

The possible spin arrangements for the 1/2-magnetization plateau with four-sublattice [○○○●○○○●…] are $\sqrt{5}a \times \sqrt{5}b$ and $2a \times 2b$ in Figs. 7(b) and 7(c), where half of the FM chains along the *b*-axis in Fig. 7(a) have changed to AF chains. Notably, for these models parallel and antiparallel spins coexist within the *ab* plane, where FM and/or AF interactions can compete with each other. The observed hysteresis between $H_{c1} < H < H_{c2}$ in Fig. 6(a) is possibly caused by the transition between different

four-sublattice states such as $\sqrt{5}a \times \sqrt{5}b$ and $2a \times 2b$, because their energy levels should be close. Above H_{c2}, saturated [○○○○○○○○…] state will appear [Fig. 7(d)]. The increase in magnetization at H_{c1} and H_{c2} is not so steep, which is typical for a powder sample with strong spin anisotropy.[37,38]

Figure 8 shows the isothermal magnetization curve for $(CrCl)LaNb_2O_7$ powder at 4.2 K. The convex curvature at low field may be due to paramagnetic impurity, as indicated by the Curie tail in the susceptibility.[26,27] The magnetization grows linearly and reaches about 2.6 μ_B at 50 T corresponding to about 63% of saturation magnetization of 4 μ_B, where $g = 2$ is assumed. The saturation field H_{sat} is expected to be around 80 T. The absence of a stepwise behavior reflects a weak anisotropy for Cr spins. Although any notable feature is not appreciable in the *M*-*H* curve, the field derivative of the magnetization d*M*/d*H* clearly shows a hump at around 12 T. This suggests a spin flop transition, as is observed for a related oxyhalide $(NiCl)Sr_2Ta_3O_{10}$[35,36] and α-$Cr_3(PO_4)_2$.[38,39] The effective field of anisotropy H_a for $(CrCl)LaNb_2O_7$ is estimated to be about 0.9 T, using mean field theory where spin flop field H_{sf} is formulated as $H_{sf} = (2H_aH_{sat})^{1/2}$.

4. Conclusion

We investigated the structure and magnetic properties of non-cupric layered oxyhalides (*M*Cl)$LaNb_2O_7$ (*M* = Mn, Co, Cr). Room-temperature TEM studies revealed the formation of two types of superstructures. NPD measurements revealed a (π 0 π) magnetic order in $(MnCl)LaNb_2O_7$ and $(CoCl)LaNb_2O_7$, as observed in

(CuBr)$LaNb_2O_7$, (CuCl)$LaTa_2O_7$ and (FeCl)$LaNb_2O_7$. Three stepwise magnetization anomalies including a 1/2 plateau between 27 T and 54 T are seen in the Co compound, which could be interpreted by a model based on the Ising model. On the other hand, (CrCl)$LaNb_2O_7$ exhibits a (π π π) magnetic order, the first observation among the ion-exchanged oxyhalide family. In these layered oxyhalides the slight difference in their crystal structures together with spin anisotropy affects their magnetism. Although in the cupric analogues FM Shastry-Sutherland models are suggested, further studies with single crystals are desired to determine magnetic models in the non-cupric (*M*Cl)$LaNb_2O_7$.

Acknowledgment

We thank M. Ichihara for helping the ED measurements. This work was supported by Grants-in-Aid for Scientific Research (A) (No. 25248016) and by Grants-in-Aid for Science Research in the Priority Areas “Novel States of Matter Induced by Frustration” (No.19052004) from the Ministry of Education, Culture, Sports, Science and Technology (MEXT), Japan. This work was also supported by Core Research for Evolutional Science and Technology (CREST) from the Japan Science and Technology Agency (JST).

1) G. Misguich and C. Lhuillier: *Frustrated Spin Systems*, (ed. H. T. Diep, World Scientific Publishing, Singapore, 2004), p. 229.
2) H. Nishimori and H. Nakanishi, J. Phys. Soc. Jpn. **57**, 626 (1986).
3) B. Bernu, P. Lecheminant, C. Lhuillier and L. Pierre, Phys. Rev. B **50**, 10048 (1994).
4) A. V. Chubukov, T. Senthil and S. Sachdev, Phys. Rev. Lett. **72** , 2089 (1994).
5) T. Itou, A. Oyamada, S. Maegawa and R. Kato, Nat. Phys. **6**, 673 (2010).
6) H. D. Zhou, E. S. Choi, G. Li, L. Balicas, C. R. Wiebe, Y. Qiu, J. R. D. Copley and J. S. Gardner, Phys. Rev. Lett. **106**, 147204 (2011).
7) N. Shannon, B. Schmidt, K. Penc and P. Thalmeier, Eur. Phys. J. B **38**, 599 (2004).
8) N. Shannon, T. Momoi and P. Sindzingre, Phys. Rev. Lett. **96**, 027213 (2006).
9) H-C. Jiang, H. Yao and L. Balents, Phys. Rev. B **86**, 024424 (2012).
~~9~~10) H. Kageyama, T. Kitano, N. Oba, M. Nishi, S. Nagai, K. Hirota, L. Viciu, J. B. Wiley, J. Yasuda, Y. Baba, Y. Ajiro and K. Yoshimura, J. Phys. Soc. Jpn. **74**, 1702 (2005).
~~10~~11) A. Kitada, Z. Hiroi, Y. Tsujimoto, T. Kitano, H. Kageyama, Y. Ajiro and K. Yoshimura, J. Phys. Soc. Jpn. **76**, 093706 (2007).
~~11~~12) Y. Tsujimoto, A. Kitada, M. Nishi, Y. Narumi, K. Kindo, T. Goko, Y. J. Uemura, A. A. Aczel, T. J. Williams, G. M. Luke, Y. Ajiro and H. Kageyama, J. Phys. Soc. Jpn. **83**, 074712 (2014).
~~12~~13) N. Oba, H. Kageyama, T. Kitano, J. Yasuda, Y. Baba, M. Nishi, K. Hirota, Y.

Narumi, M. Hagiwara, K. Kindo, T. Saito, Y. Ajiro and K. Yoshimura, J. Phys. Soc. Jpn. **75**, 113601 (2006).

~~13~~14) A. Kitada, Y. Tsujimoto, H. Kageyama, Y. Ajiro, M. Nishi, Y. Narumi, K. Kindo, M. Ichihara, Y. Ueda, Y. J. Uemura and K. Yoshimura, Phys. Rev. B **80**, 174409 (2009).

~~14~~15) Y. Tsujimoto, H. Kageyama, Y. Baba, A. Kitada, T. Yamamoto, Y. Narumi, K. Kindo, M. Nishi, J. P. Carlo, A. A. Aczel, T. J. Williams, T. Goko, G. M. Luke, Y. J. Uemura, Y. Ueda, Y. Ajiro and K. Yoshimura, Phys. Rev. B **78**, 214410 (2008).

~~15~~16) A. Kitada, Y. Tsujimoto, T. Yamamoto, Y. Kobayashi, Y. Narumi, K. Kindo, A. A. Aczel, G. M. Luke, Y. J. Uemura, Y. Kiuchi, Y. Ueda, K. Yoshimura, Y. Ajiro and H. Kageyama, J. Solid State Chem. **185**, 10 (2012).

~~16~~17) M. Yoshida, N. Ogata, M. Takigawa, J. Yamaura, M. Ichihara, T. Kitano, H. Kageyama, Y. Ajiro and K. Yoshimura, J. Phys. Soc. Jpn. **76** 104703 (2007).

~~17~~18) M. Yoshida, N. Ogata, M. Takigawa, T. Kitano, H. Kageyama, Y. Ajiro and K. Yoshimura, J. Phys. Soc. Jpn. **77**, 104705 (2008).

~~18~~19) C. Tassel, J. Kang, C. Lee, O. Hernandez, Y. Qiu, W. Paulus, E. Collet, B. Lake, T. Guidi, M. H. Whangbo, C. Ritter, H. Kageyama and S. H. Lee, Phys. Rev. Lett. **105**, 167205 (2010).

~~19~~20) A. A. Tsirlin and H. Rosner, Phys. Rev. B **82**, 060409 (2010).

~~20~~21) S. M. Yusuf, A. K. Bera, C. Ritter, Y. Tsujimoto, Y. Ajiro, H. Kageyama and J. P. Attfield, Phys. Rev. B **84**, 064407 (2011).

~~21~~22) L. Viciu, G. Caruntu, N. Royant, J. Koenig, W. L. Zhou, T. A. Kodenkandath and J. B. Wiley, Inorg. Chem. **41**, 3385 (2002).

~~22~~23) L. Viciu, J. Koenig, L. Spinu, W. L. Zhou and J. B. Wiley, Chem. Mater. **15**, 1480 (2003).

~~23~~24) N. Oba, H. Kageyama, T. Saito, M. Azuma, W. Paulus, T. Kitano, Y. Ajiro and K. Yoshimura, J. Mag. Mag. Mater. **310**, 1337 (2007).

~~24~~25) L. Viciu, J.-W. G. Bos, Y. Tsujimoto, H. Kageyama and J. B. Wiley, private communication.

~~25~~26) L. Viciu, C. O. Golub and J. B. Wiley, J. Solid State Chem. **175**, 88 (2003).

~~26~~27) A. Kitada, Y. Tsujimoto, T. Yajima, K. Yoshimura, Y. Ajiro, Y. Kobayashi and H. Kageyama, J. Phys, Conf. Ser **320**, 012035 (2011).

~~27~~28) F. Izumi and T. Ikeda, Mater. Sci. Forum **321-324**, 198 (2000).

~~28~~29) O. J. Hernandez, C. Tassel, K. Nakano, W. Paulus, C. Ritter, E. Collet, A. Kitada, K. Yoshimura and H. Kageyama, Dalton Trans. **40**, 4605 (2011).

~~29~~30) R. Melzi, P. Carretta, A. Lascialfari, M. Mambrini, M. Troyer, P. Millet and F. Mila, Phys. Rev. Lett. **85**, 1318 (2000).

~~30~~31) R. Nath, A. A. Tsirlin, H. Rosner and C. Geibel, Phys. Rev. B **78**, 064422 (2008).

~~31~~32) A. Bombardi, L. C. Chapon, I. Margiolaki, C. Mazzoli, S. Gonthier, F. Duc and P. G. Radaelli, Phys. Rev. B **71**, 220406 (2005).

~~32~~33) B. O. Loopstra, B. Van Laar and D. J. Breed, Phys. Lett. A **26**, 526 (1968).

~~33~~34) D. E. Cox, G. Shirane, B. C. Frazer and A. Narath, J. Appl. Phys. **37**, 1126 (1966).

~~34~~35) S. Furukawa, T. Dodds and Y. B. Kim, Phys. Rev. B **84**, 054432 (2011).

~~35~~36) Y. Tsujimoto, A. Kitada, Y. J. Uemura, T. Goko, A. A. Aczel, T. J. Williams, G. M. Luke, Y. Narumi, K. Kindo, M. Nishi, Y. Ajiro, K. Yoshimura and H. Kageyama, Chem. Mater. **22**, 4625 (2010).

~~36~~37) T. Oguchi, J. Phys. Soc. Jpn. **20**, 2236 (1965).

~~37~~38) H. Kageyama, K. Yoshimura, K. Kosuge, M. Azuma, M. Takano, H. Mitamura and T. Goto, J. Phys. Soc. Jpn. **66**, 3996 (1997).

~~38~~39) A. N. Vasiliev, O. S. Volkova, E. Hammer, R. Glaum, J.-M. Broto, M. Millot, G. Nénert, Y. T. Liu, J.-Y. Lin, R. Klingeler, M. Abdel-Hafiez, Y. Krupskaya, A. U. B. Wolter, and B. Büchner, Phys. Rev. B **85**, 014415 (2012).

Fig. 1. (a) Crystal structure for (*M*Cl)$LaNb_2O_7$ (*M* = Cu, V, Fe, Mn, Co, Cr). (b, c) Antiferromagnetic order with the modulation vector q_{mag} = (π 0), observed in *M* = Mn and Co (b) and q_{mag} = (π π), observed in *M* = Cr (c), where arrows represent spins.

Fig. 2. Electron diffraction patterns along [001] for (a) *M* = Mn, (b) Co and (c) Cr, in which each supercell is shown by dashed lines.

Fig. 3. Neutron powder diffraction profiles of (*M*Cl)$LaNb_2O_7$ for (a) *M* = Mn (b) Co and (c) Cr, collected at above and below T_N.

Fig. 4. Temperature dependence of the intensity of the (1/2 0 1/2) reflection for (a) *M* = Mn and (b) Co. (c) Temperature dependence of the intensity of the (1/2 1/2 1/2) reflection for *M* = Cr. The solid curves are guide to the eyes.

Fig. 5. Observed (closed circles) versus calculated (solid curves) NPD profiles of (a) *M* = Mn (b) Co and (c) Cr. Solid curves in (a)-(c) show the simulated intensities with the *c*-axis spin orientation (upper panel) and the *b*-axis spin orientation (lower panel). In all cases, profiles with the *c*-axis spin orientation gave better fits (see text for details).

Fig. 6. (a) Magnetization curve of (CoCl)$LaNb_2O_7$ measured at 1.3 K (solid curves), demonstrating two-step metamagnetic transitions at H_{c1} = 27 T and H_{c2} = 54 T. Dashed and dot-dashed lines assume the magnetization parallel and perpendicular to the easy-axis ($M_{//}$ and $M_{\perp}$), respectively. A ferromagnetic component (M_{FM}) is indicated. (b) A possible easy-axis magnetization curve for (CoCl)$LaNb_2O_7$. Open and closed circles represent up and down spins, respectively.

Fig. 7. Possible magnetic structures of (CoCl)$LaNb_2O_7$: (a) $2a \times b$ with $M_{//} = 0$ at $0 < H < 5$ T, (b) $\sqrt{5}a \times \sqrt{5}b$ and (c) $2a \times 2b$ with $M_{//} = 1/2M_{//sat}$ at $H_{c1} < H < H_{c2}$, and (d) $a \times b$ with $M_{//} = M_{//sat}$ above H_{c2}. Each magnetic unit cell is shown by shaded area.

Fig. 8. Magnetization curves *M* (upper panel) and differential magnetization curves d*M*/d*H* (lower panel) for (CrCl)$LaNb_2O_7$ measured at 4.2 K. Dashed lines are guide to eyes.

Table I. The temperatures where the susceptibilities have broad maxima (T^{χ}_{max}), the Weiss temperature (θ) and the suggested antiferromagnetic transition temperatures (T_N) for (MCl)$LaNb_2O_7$ reported previously.[22, 26]

Compound	T^{χ}_{max} (K)	θ (K)	T_N (K)
(FeCl)$LaNb_2O_7$	87	−151.5	78
(MnCl)$LaNb_2O_7$	65	−131	53
(CoCl)$LaNb_2O_7$	67	−77.95	61
(CrCl)$LaNb_2O_7$	55	−61	52

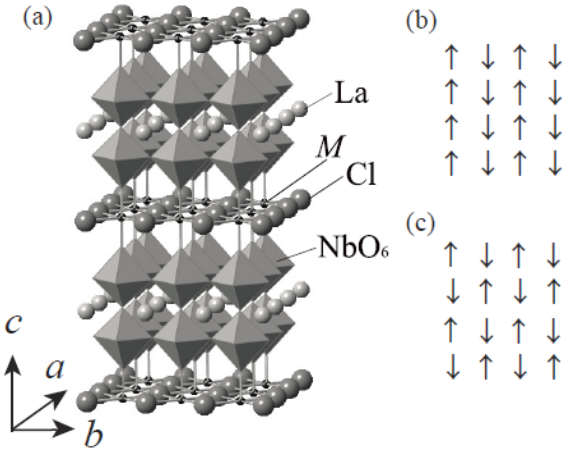

Fig. 1 A. Kitada *et al.*

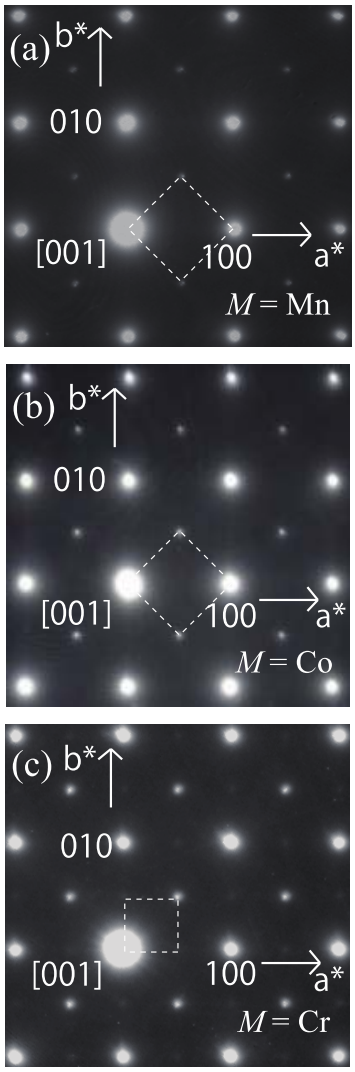

Fig. 2 A. Kitada *et al*.

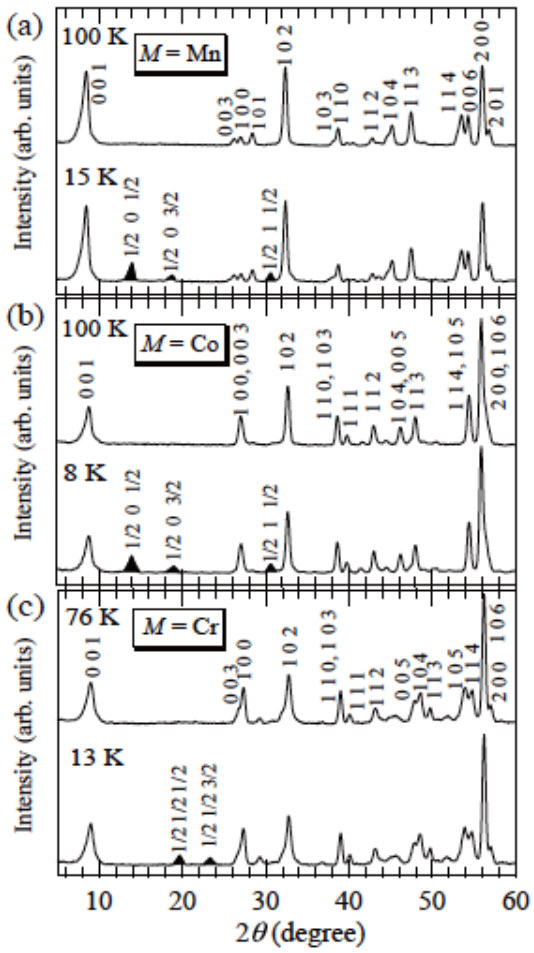

Fig. 3 A. Kitada *et al.*

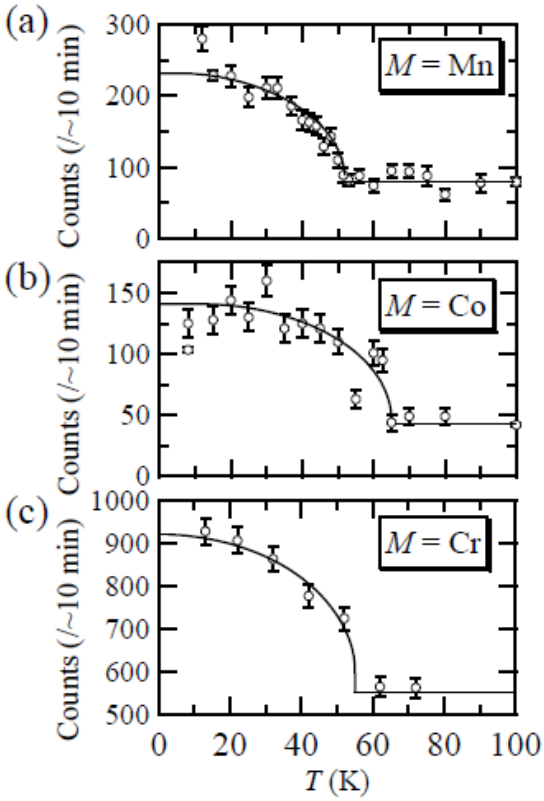

Fig. 4 A. Kitada *et al.*

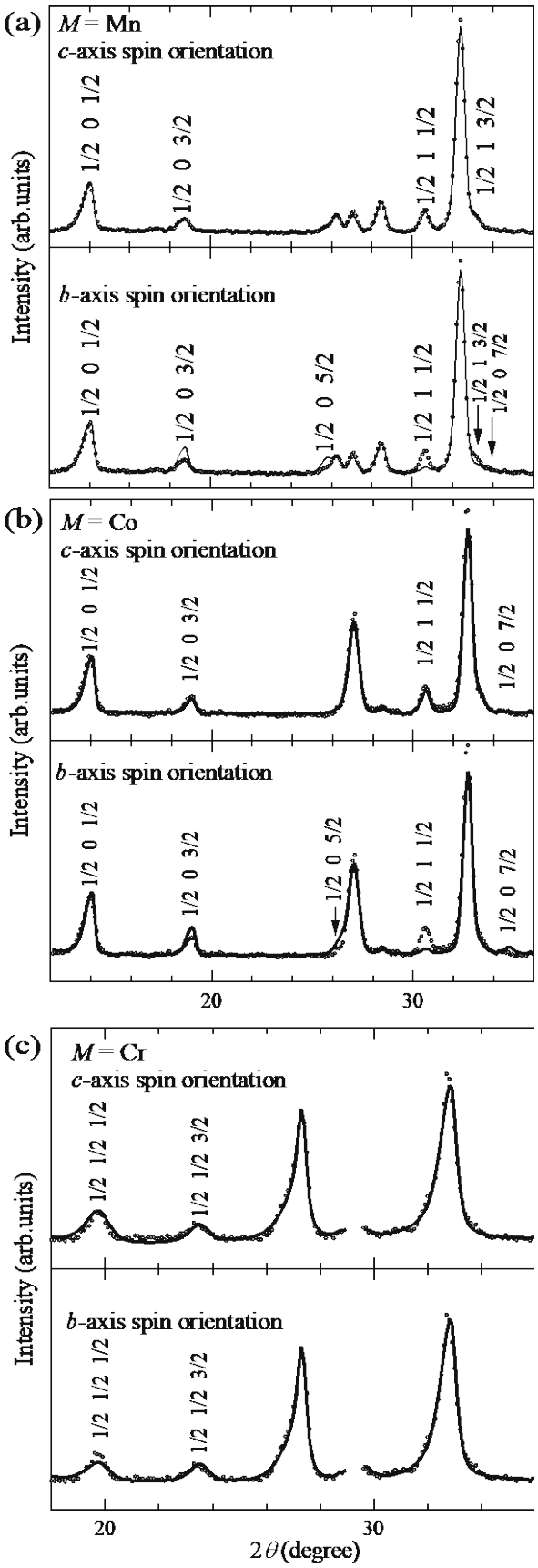

Fig. 5 A. Kitada *et al.*

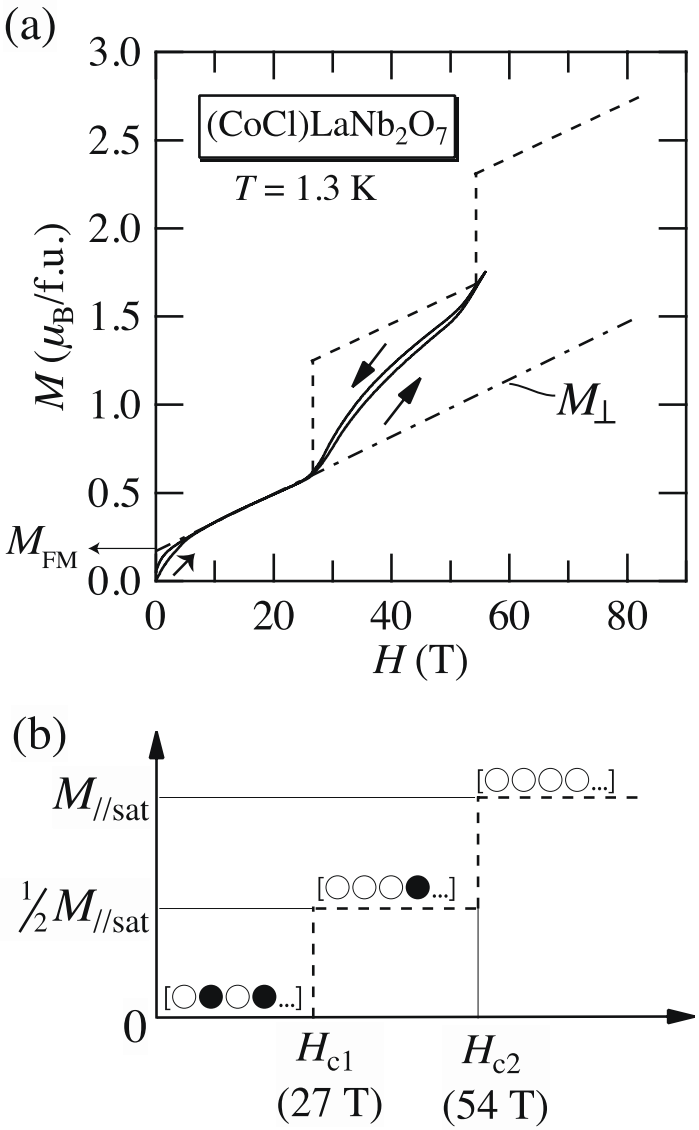

Fig. 6 A. Kitada *et al*.

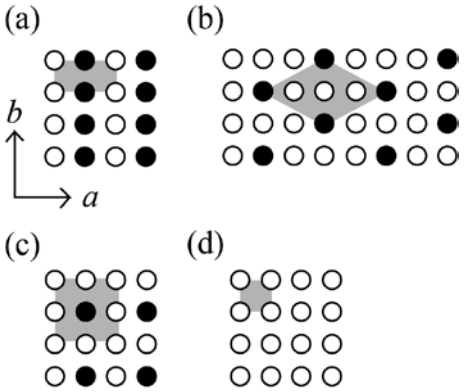

Fig. 7 A. Kitada *et al.*

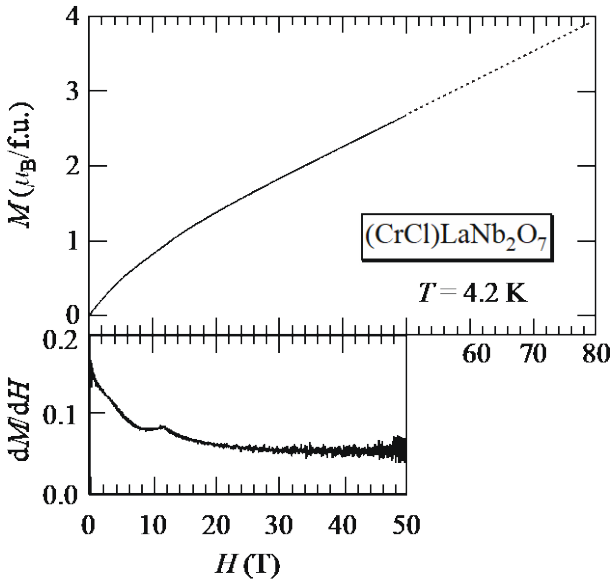

Fig. 8 A. Kitada *et al.*